NASA/TM-20240003569

Demonstration of GaN HEMT MMIC High-Power Amplifier for Lunar Proximity Communications

Rainee N. Simons, Marie T. Piasecki, Joseph A. Downey, and Bryan L. Schoenholz
Glenn Research Center, Cleveland, Ohio

Mansoor K. Siddiqui
Northrop Grumman Aerospace Systems, Redondo Beach, California

April 2024

NASA STI Program Report Series

Since its founding, NASA has been dedicated to the advancement of aeronautics and space science. The NASA scientific and technical information (STI) program plays a key part in helping NASA maintain this important role.

The NASA STI program operates under the auspices of the Agency Chief Information Officer. It collects, organizes, provides for archiving, and disseminates NASA's STI. The NASA STI program provides access to the NTRS Registered and its public interface, the NASA Technical Reports Server, thus providing one of the largest collections of aeronautical and space science STI in the world. Results are published in both non-NASA channels and by NASA in the NASA STI Report Series, which includes the following report types:

- TECHNICAL PUBLICATION.
  Reports of completed research or a major significant phase of research that present the results of NASA Programs and include extensive data or theoretical analysis. Includes compilations of significant scientific and technical data and information deemed to be of continuing reference value. NASA counterpart of peer-reviewed formal professional papers but has less stringent limitations on manuscript length and extent of graphic presentations.

- TECHNICAL MEMORANDUM.
  Scientific and technical findings that are preliminary or of specialized interest, e.g., quick release reports, working papers, and bibliographies that contain minimal annotation. Does not contain extensive analysis.

- CONTRACTOR REPORT.
  Scientific and technical findings by NASA-sponsored contractors and grantees.

- CONTRACTOR REPORT.
  Scientific and technical findings by NASA-sponsored contractors and grantees.

- CONFERENCE PUBLICATION.
  Collected papers from scientific and technical conferences, symposia, seminars, or other meetings sponsored or co-sponsored by NASA.

- SPECIAL PUBLICATION.
  Scientific, technical, or historical information from NASA programs, projects, and missions, often concerned with subjects having substantial public interest.

- TECHNICAL TRANSLATION.
  English-language translations of foreign scientific and technical material pertinent to NASA's mission.

Specialized services also include organizing and publishing research results, distributing specialized research announcements and feeds, providing information desk and personal search support, and enabling data exchange services.

For more information about the NASA STI program, see the following:

- Access the NASA STI program home page at http://www.sti.nasa.gov

NASA/TM-20240003569

Demonstration of GaN HEMT MMIC High-Power Amplifier for Lunar Proximity Communications

Rainee N. Simons, Marie T. Piasecki, Joseph A. Downey, and Bryan L. Schoenholz
Glenn Research Center, Cleveland, Ohio

Mansoor K. Siddiqui
Northrop Grumman Aerospace Systems, Redondo Beach, California

Prepared for the
Space Hardware and Radio Conference (SHaRC)
cosponsored by IEEE and MTT-S
San Antonio, Texas, January 21–24, 2024

National Aeronautics and
Space Administration

Glenn Research Center
Cleveland, Ohio 44135

April 2024

Acknowledgments

The authors would like to thank Nicholas Varaljay for installing the DC bias harness on the HPAs and the Space Communications and Navigation (SCaN) Program for their support. This NASA Technical Memorandum (TM) is an expanded version of the Space Hardware and Radio Conference paper that was presented at Radio and Wireless Week in San Antonio, Texas, from January 21 to 24, 2024. The Figures for this NASA TM are archived under E-20158 and E-20215. The GaN MMIC power amplifier modules were procured from Northrop Grumman under order number 80NSSC20P1729. The characterization of the modules were performed at NASA Glenn Research Center in support of a contract awarded to Northrop Grumman (80NSSC21P2024) entitled “Feasibility Study of a Ka-band Solid-State High-Power Amplifier-Phase A.”

Level of Review: This material has been technically reviewed by technical management.

This report is available in electronic form at https://www.sti.nasa.gov/ and https://ntrs.nasa.gov/

NASA STI Program/Mail Stop 050
NASA Langley Research Center
Hampton, VA 23681-2199

Demonstration of GaN HEMT MMIC High-Power Amplifier for Lunar Proximity Communications

Rainee N. Simons, Marie T. Piasecki, Joseph A. Downey, and Bryan L. Schoenholz
National Aeronautics and Space Administration
Glenn Research Center
Cleveland, Ohio 44135

Mansoor K. Siddiqui
Northrop Grumman Aerospace Systems
Redondo Beach, California 90278

Abstract

In this paper, we demonstrate a high efficiency, Ka-band (23.15 to 23.55 GHz) GaN HEMT MMIC based single-ended high power amplifier (HPA). The measured P_{out}, Gain, PAE, RMS EVM for Offset-QPSK, 8PSK, 16APSK, and 32APSK waveforms, 3rd-order IMD products, noise figure, and phase noise are presented. The results indicate that the saturated output power (P_{sat}) and the small signal Gain are on the order of 38.8 dBm (7.6 W) and 29.3 dB, respectively. The PAE at P_{sat} is 20.0%. At the 1-dB compression point, the RMS EVM and the out-of-band spectral regrowth are less than 6% and –26 dBc respectively, for all four waveforms. Additionally, the spectrum is in compliance with the NTIA mask requirements for all four waveforms. The output 3rd-order intercept point (OIP3) is on the order of 42 dBm. The noise figure is less than 9.5 dB. The SSB phase noise spectral density is compliant with the envelope defined by the MIL-STD-188-164C. The HPA can enable proximity forward links between the orbiting Gateway/relay satellites and the lunar surface elements and cross links between relay satellites.

Introduction

The vision for NASA's Artemis mission is to enable human/robotic exploration of the Moon's surface/interior and provide a long-term presence on the Moon. To achieve this vision, NASA plans to develop a lunar Gateway to serve as an outpost, human landing systems and ascent elements for transporting the astronauts to and from the lunar surface, relay satellites for communications, surface habitats, terrain vehicles, and rovers for exploring the lunar landscape (Ref. 1). Additionally, NASA plan to use the commercial lunar payload services (CLPS) initiative for the transportation and deployment of science instruments and other payloads on the lunar surface (Ref. 2). In the above missions, to ensure astronaut's health and safety and for transferring science data from surface instruments to Earth, NASA plans to deploy robust communication links between the lunar surface elements such as, the landers, habitats, terrain vehicles, rovers, and the orbiting Gateway/relay satellites and as illustrated in Figure 1.

This paper builds on our prior and ongoing efforts in the development of Ka-band high efficiency gallium nitride (GaN) monolithic microwave integrated circuit (MMIC) based high-power amplifiers (HPAs). In these HPAs, the MMICs utilize GaN high electron mobility transistor (HEMT) technology that imparts several significant advantages over prior gallium arsenide (GaAs), Silicon Germanium (SiGe) and Silicon (Si) technologies. These include higher operating voltage, higher output power density, higher channel operating temperatures, and radiation hardness (Refs. 3 to 9). Additionally, the technology, topology, device features, and RF performance characteristics of recent K- and Ka-band GaN MMIC based SSPAs presented in References 5 to 9 are summarized in Table I.

NASA's Projected Concept of Operation and Architecture (PCOA) for Space Communication and Navigation (SCaN) Networks for the next decade or two plans to use open and international standards to ensure interoperability and link connections that have potential to support cognitive for optimizing throughput (Ref. 10). In view of the above, we recently demonstrated a prototype of a switched wideband GaN HEMT based MMIC HPA that operates across the 25.25 to 31 GHz frequency band for user spacecraft terminals to support interoperability (Ref. 11). Additionally, we investigated the benefits offered by GaN HPA's performance characteristics for user spacecraft cognitive radio platforms (Ref. 12).

In this paper, we extend the above developments to the design and demonstration of a 23.15 to 23.55 GHz GaN HEMT based MMIC HPA. The HPA's performance is demonstrated in the context of future lunar proximity communication forward links that are planned between assets located in the lunar orbit and lunar surface, cross links between lunar relays, and links to science mission spacecraft. The electromagnetic spectrum requirements for these links are presented in Table II. The performance of the 27 to 27.5 GHz HPA for the corresponding return links is presented in Reference 11.

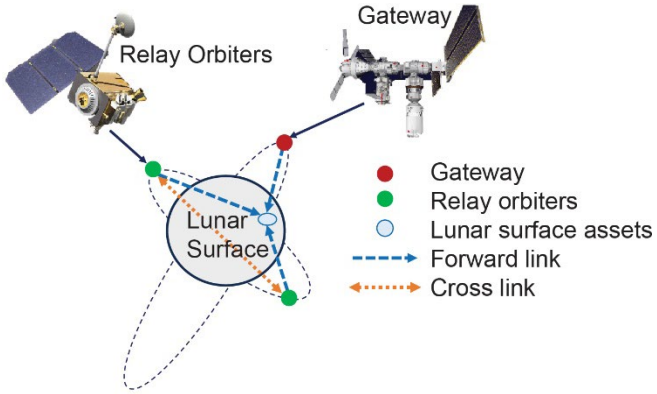

Figure 1.—Ka-Band High-Rate Lunar System Proximity Links.

TABLE I.—STATE-OF-THE-ART OF K-BAND AND Ka-BAND GaN MMIC BASED SOLID-STATE POWER AMPLIFIERS (SSPAs)

Reference	Technology	Device	Frequency, GHz	Topology	SSPA				Applications
					P_{sat}	Linear gain or Small signal gain, dB	PAE, percent	Size and Mass	
5	Northrop Grumman Aerospace Systems foundry, GaN20 process (US)	0.2 μm gate length, 3-stage architecture, total gate periphery 1.84 mm, chip size: 5.4 x 3.1 mm,100 μm thick SiC, chip P_{out} = 10 W	31 to 34	4-way power divider/combiner realized with binary 2-tier waveguide H-plane junctions, input/output ports are WR-22 waveguide	45.1 dBm (32.4 W CW) at 32.5 GHz and V_{ds} = 28 V	25	30	3.45 x 2.34 x 1.25 in. (87.6 x 59.4 x 31.8 mm) and 2.2 lb (1 Kg)	Satellite downlinks
6	Qorvo GaN QGaN15 process (US)	0.15 μm gate length, 3-stage architecture, QPA2211D MMIC, die size: 2.74 x 2.55 x 0.05 mm, SiC substrate, chip P_{out} = 14 W with 25% PAE at 25 °C	27 to 31	16-way Spatium divider/ combiner, 2.92 mm coax connector at input port and WR-28 waveguide at output port	50 dBm (100 W CW) at 71 °C, V_{ds} = 22 V and total I_{ds} = ~5A (~300 mA x 16)	23	17%	4 x 3 x 3.25 in. (101.6 x 76.2 x 82.6 mm), Mass not available	Commercial SatCom uplink
7	United Monolithic Semiconductors, GaN GH15-10 technology (France)	0.15 μm gate length, 3-stage architecture, chip size: 5 x 3.5 mm, 70 μm thick SiC, chip P_{out} = 10 W	17.3 to 20.2	4-way divider/combiner using a magic-tee configuration, input/output ports are waveguide WR-51	46 dBm (39.8 W CW) across 17.3 to 20.2 GHz	50	NA	Breadboard	New GEO/MEO satellite communication services
8	Fraunhofer Institute for Applied Solid State Physics (IAF), GaN10 technology (Germany)	0.1 μm gate length, 3-stage architecture, 8 finger HEMT device with a unit gate width of 60 μm, chip size: 4 x 3.5 mm, 75 μm thick SiC, chip P_{out} = 10 W	28 to 38	16-way radial splitter/combiner combines the output of the 16 self-contained modules, each module features split-block construction with biasing circuitry, connections to MMIC via E-field probes, and WR-28 waveguide input/output ports	>50 dBm (>100 W CW), V_{ds} = 15 V and total I_{ds} for 16 modules plus one driver module = 33.6 A	>20	>20	System diameter is 6.46 in. (164 mm), Mass not available	Multiband communication terminals and high-power measurement equipment
9	MACOM European Semiconductor Center (MESC) GaN-on-Si technology (France)	0.1 μm gate length, 3-stage architecture, chip size: 5 x 4.4 mm, chip P_{out} = 10 W	17.3 to 20.2	16-way cavity based radial splitter/combiner with WR-42 waveguide ports	>50 dBm (>100 W CW), V_{ds} = 9 V	70	>22	12.44 x 9.13 x 3.3 in. (316 x 232 x 83.9 mm), 8 lb (3.62 Kg)	Very-high-throughput satellite downlinks

TABLE II.—ELECTROMAGNETIC SPECTRUM FOR LUNAR PROXIMITY REGION

Links	Forward link frequency, GHz	Return link frequency, GHz
Lunar Orbit to Lunar Surface	23.15 to 23.55	----------
Lunar Surface to Lunar Orbit	----------	27 to 27.5
Lunar Orbit to Lunar Orbit Relay Cross Link	23.15 to 23.55	27 to 27.5
Lunar Orbit to Lunar Orbit Science Mission Link	23.15 to 23.55	27 to 27.5

HPA Design and Brief Set of Specifications

The two-stage GaN MMIC driver and power amplifier chips used in the demonstration are shown in Figure 2(a) and (b), respectively. In these chips, the devices are fabricated with 0.2 µm T-gates on GaN HEMT epitaxial layers that are grown on 4H-SiC wafers. The SiC wafers are thinned to 100 µm for efficient waste heat removal and their backside is gold plated for compatibility with eutectic bonding. A SiN passivation film is applied to the chip surface to reduce the effect of interface traps and improve reliability. To demonstrate microwave performance, the driver amplifier chip and the power amplifier chip are assembled into two separate modules. The modules are interconnected to realize a prototype single-ended HPA, as shown in Figure 3, and overall performance characterized. Brief set of specifications are:

- Forward link frequency range: 23.15 to 23.55 GHz
- Output saturated power (P_{sat}): 7.5 to10 W (CW)
- Power added efficiency at P_{sat} (PAE): 20 to 25%
- Small signal Gain (drive & power amplifier): >25 dB
- RMS Error Vector Magnitude (RMS EVM): <6%
- Gain flatness: ±1 dB
- Input/output return loss: <10.0 dB

Ka-Band High Power Amplifier Performance Validation

The performance of the HPA is characterized using Rohde & Schwarz (R&S) SMW200A Vector Signal Generator (VSG), R&S FSW Signal and Spectrum Analyzer, Micronetics Noise Source, and Keysight N6705C DC Power Analyzer. The driver amplifier was initially characterized to ensure linear operation throughout the experiments below.

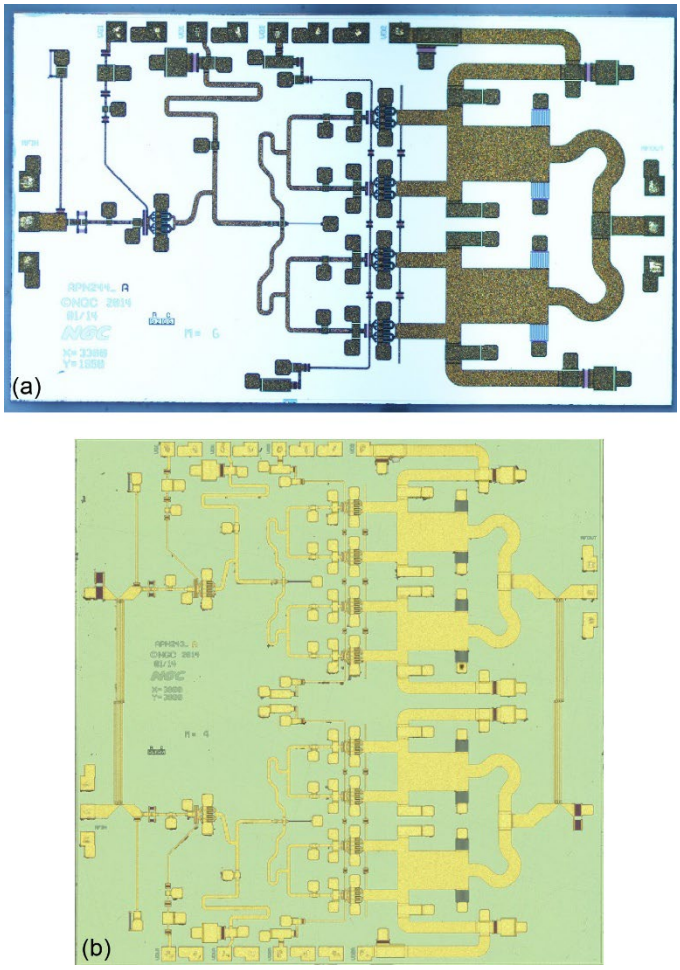

Figure 2.—GaN MMIC Chips. (a) Driver Amplifier (APN244) (Die size: 3.3 x 1.95 mm). (b) Power Amplifier (APN243) (Die size: 3.8 x 3.8 mm).

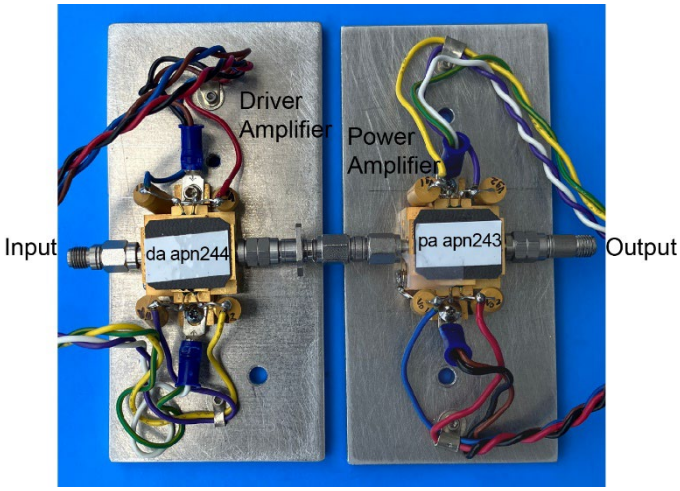

Figure 3.—Prototype single-ended HPA with interconnected GaN MMIC driver and power amplifier modules. The GaN MMIC driver and power amplifier chips are Northrop Grumman APN244 and APN243, respectively.

Driver Amplifier Output Power, Gain, and PAE

The measured P_{out}, Gain, and PAE of the driver amplifier module at the center frequency (f_0) of 23.35 GHz are presented in Figure 4(a) and (b), respectively. The saturated output power (P_{sat}) and the small signal Gain are on the order of 31.81 dBm (1.52 W) and 17 dB, respectively. The PAE at P_{sat} is 17%. A similar set of results have been obtained at the lower and upper band edge frequencies and summarized in Table III.

TABLE III.—DRIVER AMPLIFIER MODULE MEASURED P_{sat}, GAIN, AND PAE AS A FUNCTION OF FREQUENCY

Frequency, GHz	P_{sat}, dBm	Small signal gain, dB	PAE, percent
23.0	31.64	17.25	17.03
23.35	31.81	17.0	17
23.6	31.69	17.8	16.8

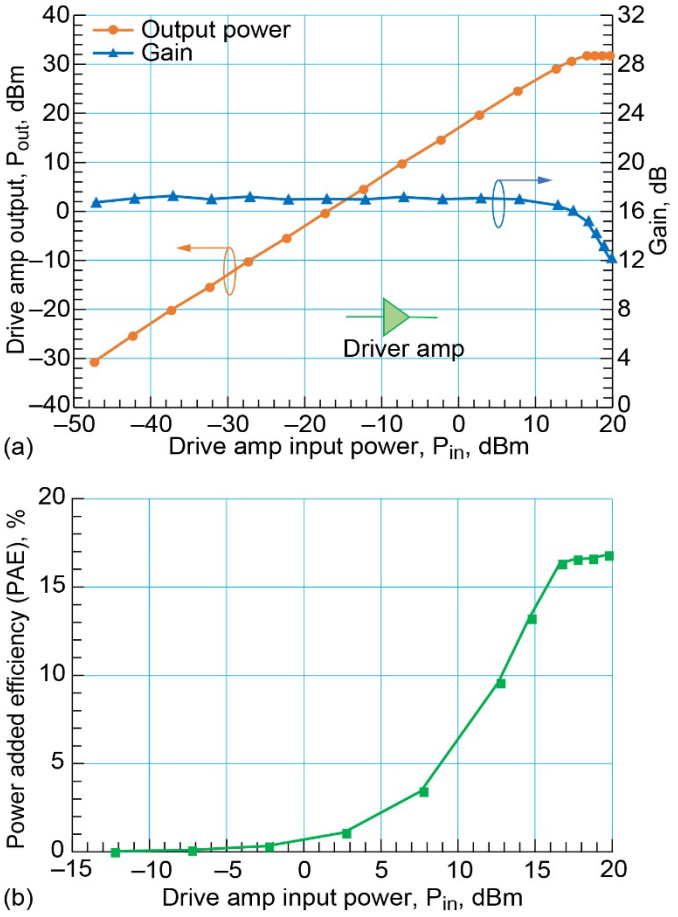

Figure 4.—(a) Measured P_{out} and Gain versus P_{in} of the driver amplifier (APN244) module at f_0 of 23.35 GHz. $V_{d1} = V_{d2} =$ 23.1 V, $I_{d1} = 0.070$ A, $I_{d2} = 0.344$ A, and $V_{g1} = V_{g2} = -3.9$ V. (b) Power added efficiency versus P_{in}. T = 25 °C (Note: The above curent values are at saturation and no attempts were made to optimize the drain/gate voltages).

HPA Output Power, Gain, and PAE

The measured P_{out}, Gain, and PAE at the carrier or center frequency (f_0) of 23.35 GHz for the interconnected driver and power amplifier modules are presented in Figure 5(a) and (b), respectively. The P_{sat} and the small signal Gain are on the order of 38.8 dBm (7.6 W) and 29.3 dB, respectively. The PAE at P_{sat} is 20.0%. A similar set of results have been obtained at the lower and upper band edge frequencies of 23.15 and 23.55 GHz, respectively. To obtain P_{sat} greater than 38.8 dBm, two power amplifiers and a driver amplifier can be arranged in a balanced configuration as demonstrated in Reference 12.

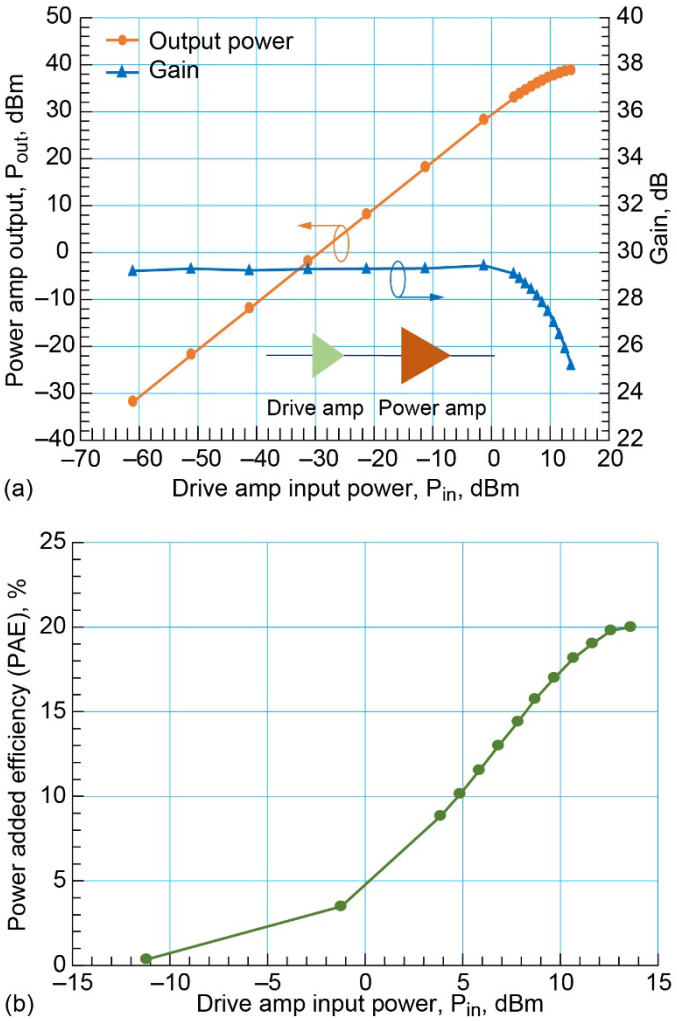

Figure 5.—(a) Measured P_{out} and Gain versus P_{in} of the interconnected driver (APN244) and power amplifier (APN243) modules at f_0 of 23.35 GHz. Driver amplifier: $V_{d1} = V_{d2} =$ 23.1 V, $I_{d1} = 0.069$ A, $I_{d2} = 0.321$ A, and $V_{g1} = V_{g2} = -3.9$ V. Power amplifier: $V_{d1} = V_{d2} = 23$ V, $I_{d1} = 0.23$ A, $I_{d2} =$ 1.03 A, and $V_{g1} = V_{g2} = -4.5$ V. (b) Power added efficiency versus P_{in}. T = 25 °C (Note: The above current values are at saturation and no attempts were made to optimize the drain/gate voltages).

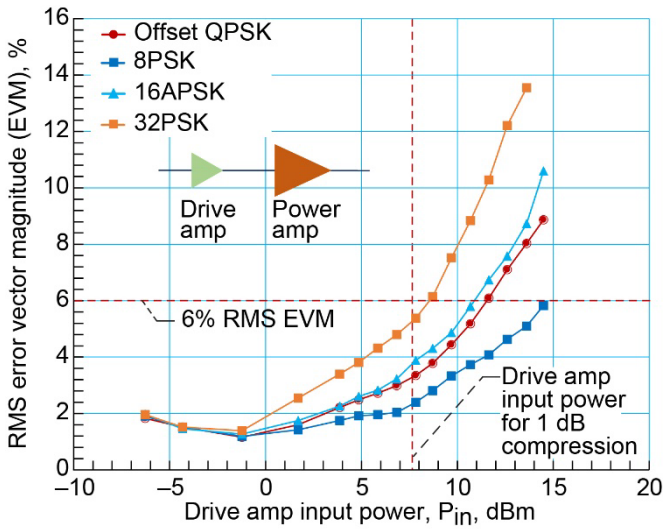

Figure 6.—Measured RMS EVM versus P_{in} at f_0 of 23.35 GHz. The symbol rate is 180 Msymbols per second and square root raised cosine (SRRC) filter is set to 0.35.

HPA RMS Error Vector Magnitude (RMS EVM)

To demonstrate high data rate and bandwidth efficiency, the RMS EVM is measured at a fixed rate of 180 Msymbols per second for the Offset-QPSK, 8PSK, 16APSK, and 32APSK waveforms that are typically used in the transmission of data in satellite communications. The results achieved are presented in Figure 6. At the 1-dB compression point, all waveforms can achieve RMS EVM of <6%. The measured spectrum for all four waveforms, when P_{in} is close to the 1-dB compression point, are presented in Figure 7. The results indicate that the spectral efficiency for a fixed bandwidth (225 MHz) increases from 2 to 5 bits/s/Hz. Additionally, the spectrum is compliant with the NTIA mask (Ref. 13). Furthermore, the out-of-band spectral regrowth measured at 1-symbol rate (180 MHz) away from the carrier or center frequency (f_0 = 23.35 GHz) for all four waveforms is less than –26 dBc, which shows that the adjacent channel interference or adjacent channel power ratio (ACPR) is small.

HPA 3rd-order Intermodulation Distortion (IMD)

In Figure 8, the measured 3rd-order intermodulation distortion products are presented to demonstrate good linearity. The data indicates that the output 3rd-order intercept point (OIP3) is on the order of 42 dBm.

HPA Noise Figure (NF) and Associated Gain

The measured NF and associated gain are presented in Figure 9. The NF and the associated gain are on the order of <9.5 and 29 dB, respectively, across the 23.15 to 23.55 GHz range.

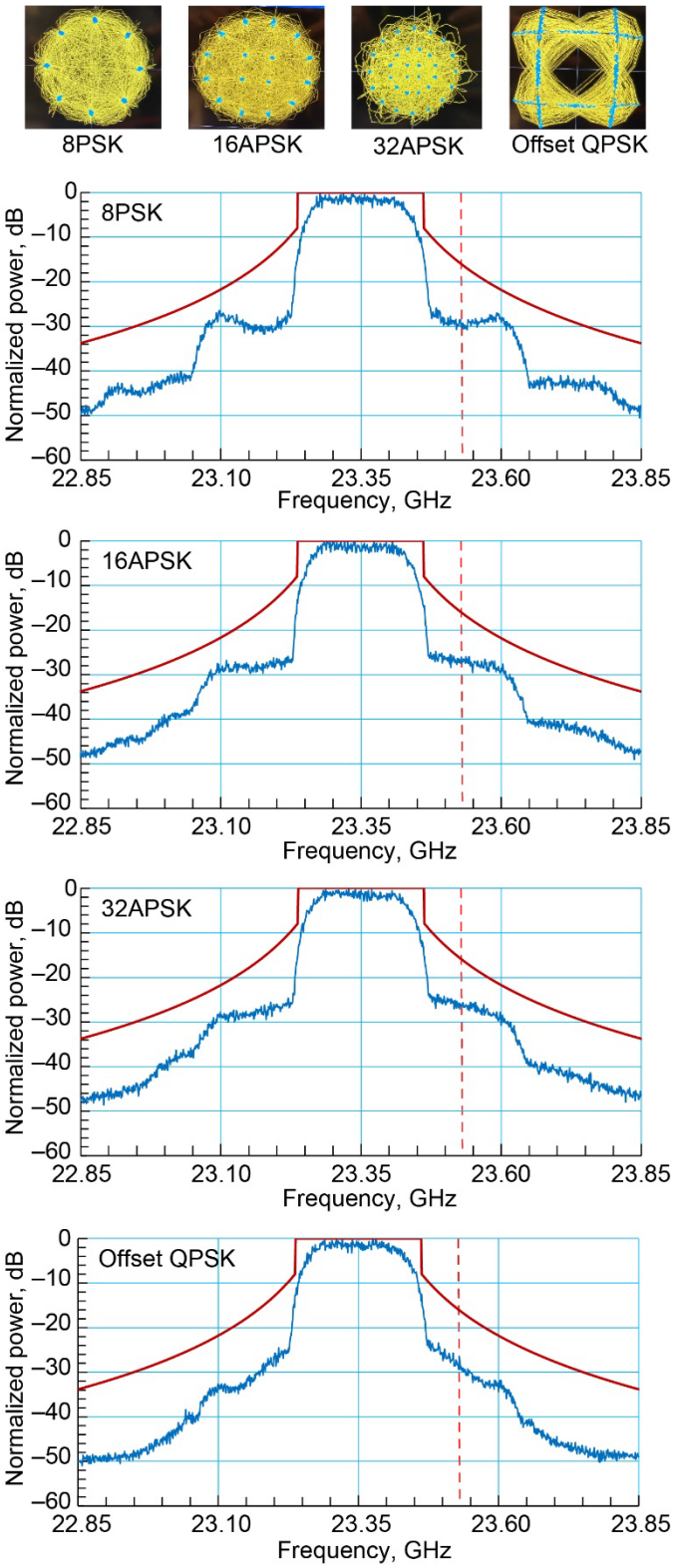

Figure 7.—Measured spectrum for 8PSK, 16APSK, 32APSK, and Offset-QPSK, waveforms at f_0 of 23.35 GHz. Symbol rate is 180 Msymbols per second, SRRC filter is set to 0.35, and bandwidth is 225 MHz. The red solid line is the NTIA emission mask.

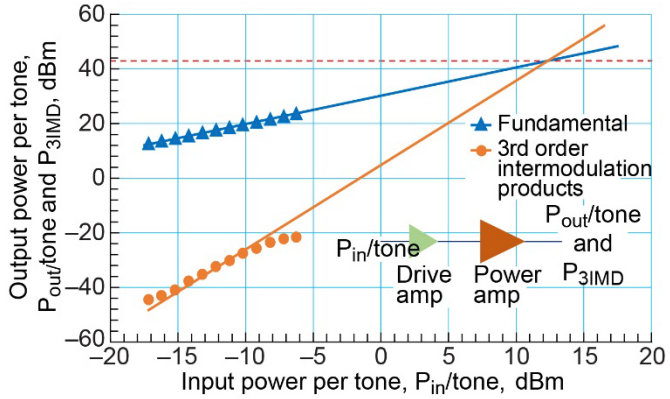

Figure 8.—Measured 3rd-order intermodulation distortion (IMD) versus input power per tone. Tone frequencies are f_0 = 23.35 GHz ±2.5 MHz. Tone spacing is 5 MHz.

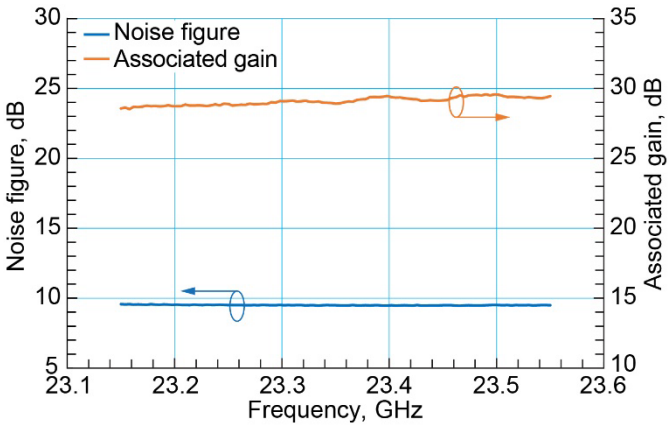

Figure 9.—Measured noise figure and associated gain versus frequency.

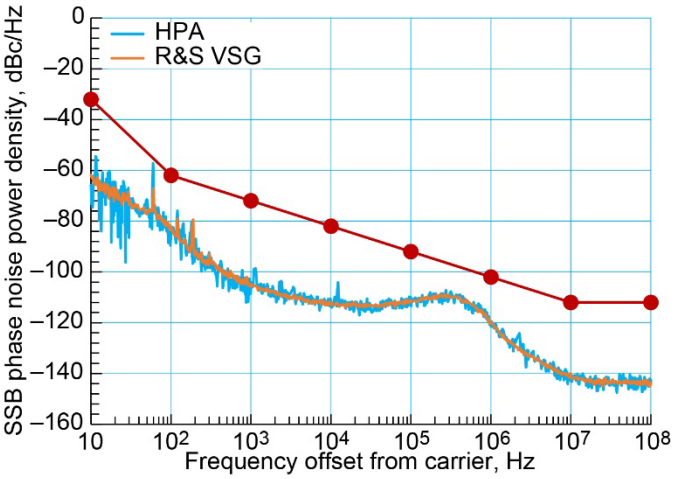

Figure 10.—Measured SSB Phase Noise spectral power density versus the frequency offset from the carrier frequency. The carrier frequency is 23.35 GHz. The red solid line is the MIL-STD-188-164C. The superimposed blue and orange traces are the SSB Phase Noise characteristics of the HPA and R&S VSG, respectively.

HPA Single Sideband (SSB) Phase Noise

The measured SSB phase noise spectral density is presented in Figure 10. The SSB phase noise spectral density is compliant with the envelope defined by the MIL-STD-188-164C. When compared with the carrier signal from the R&S VSG, the phase noise of the amplified signal near the carrier is not degraded by the HPA.

Conclusions and Discussions

The advantages of GaN HPAs for NASA's lunar proximity communication applications are highlighted. The design and brief specifications for a 23.15 to 23.55 GHz GaN HEMT MMIC based HPA is presented. The design is validated by characterizing the prototype single-ended HPA. The measured P_{sat}, Gain, PAE, RMS EVM for Offset-QPSK, 8PSK, 16APSK, and 32APSK waveforms, spectrum, out-of-band spectral regrowth, 3rd-order IMD intercept point, NF, and phase noise are presented and summarized in Table IV. No de-rating of the GaN MMIC chips is done. However, preliminary thermal analysis to estimate junction temperature and projected lifetime are provided in References 3 and 14. The above HPA development is at technology readiness level of 4 (TRL 4). GaN HEMTS enable higher power density, higher PAE resulting in lighter, smaller, and more efficient RF/microwave systems in contrast with Si, SiGe, and GaAs based systems.

TABLE IV.—SUMMARY OF HPA TEST RESULTS

Parameter	Measured value
Carrier or Center Frequency (GHz)	23.35
Saturated Output Power (P_{sat}) (dBm)	38.8 (7.6 W)
Small Signal Gain (dB)	29.3
Peak PAE (%)	20.0
Return Loss (dB)	< –10.0
RMS EVM for Offset-QPSK, 8PSK, 16APSK, and 32APSK waveforms (P_{in} is at the 1-dB compression point) (%)	<6
Out-of-Band Spectral Regrowth (dBc)	< –26.0
OIP3 (dBm)	42.0
Noise Figure (dB)	<9.5
SSB Phase Noise Spectral Power Density (dBc/Hz) (P_{in} is at the 1-dB compression point)	Compliant with MIL-STD Mask

References

1. NASA's Artemis Program, https://www.nasa.gov/artemisprogram.
2. NASA's Commercial Payload Services Initiative, https://www.nasa.gov/commercial-lunar-payload-services/
3. S. Din, M. Wojtowicz and M. Siddiqui, "High Power and High Efficiency Ka-band Power Amplifier," *IEEE MTT-S Inter. Micro Symp Dig*, Phoenix, AZ, May 17–22, 2015.
4. S. Din, A.M. Morishita, N. Yamamoto, C. Brown, M. Wojtowicz, and M. Siddiqui, "High-Power K-Band GaN PA MMICs and Module for NPR and PAE," *IEEE MTT-S Inter. Micro Symp Dig*, Honololu, HI, June 4–9, 2017.
5. N. Estella, E. Camargo, J. Schellenberg, and L. Bui, "High-efficiency, Ka-Band GaN Power Amplifiers," *IEEE MTT-S Inter. Micro Symp Dig*, Boston, MA, June 2–7, 2019.
6. S.D. Yoon, J. Kitt, D. Murdock, E. Jackson, M. Roberg, G. Hegazi, and P. Courtney, "Highly Linear & Efficient Power Spatium Combiner Amplifier with GaN HPA MMIC at Millimeter Wavelength Frequency," *IEEE MTT-S Inter. Micro Symp Dig*, Los Angeles, CA, Aug. 4–6, 2020.
7. A. Maati, G. Mouchon, J. Belluot, P. Augoyat, M. Dinari, T. Huet, V. Serru, M. Camiade, and A. Katz, "Design and Characterization of a Ka Band 40 W RF Chain Based on GH15-10 GaN Technology for Space Solid State Power Amplifier Applications," *Proc. 50th European Microwave Conf.*, Utrecht, The Netherlands, Jan. 12–14, 2021.
8. P. Neininger, L. John, M. Zink, D. Meder, M. Kuri, A. Tessmann, C. Friesicke, M. Mikulla, R. Quay, and T. Zwick, "Broadband 100-W Ka-Band SSPA Based on GaN Power Amplifiers," *IEEE Microwave and Wireless Components Lett.*, vol. 32, no. 6, pp. 708–711, June 2022.
9. R. Giofre, L. Cabria, R. Leblanc, M. Lopez, F. Vitobello, and P. Colantonio, "An Efficient and Linear SSPA with Embedded Power Flexibility for Ka-Band Downlink SatCom Applications," *IEEE Trans. Microwave Theory and Techniques,* vol. 72, no. 1, pp. 563–574, Jan 2024.
10. Space Communications and Navigation (SCaN) Network Projected Concept of Operations and Architecture (PCOA), Section 3, NASA Headquarters, Washington, D.C., Feb. 16, 2023.
11. R.N. Simons, J.A. Downey, B.L. Schoenholz, M.T. Piasecki, N.T. Pham, M.K. Siddiqui, and R.G. Bonnin, "Demonstration of a Switched Wideband GaN High-Power Amplifier for Future Space Missions," *2023 IEEE Space Hardware and Radio Conference*, Las Vegas, NV, Jan. 22–25, 2023.
12. R.N. Simons, A.M. Gannon, J.A. Downey, M.T. Piasecki, and B.L. Schoenholz, "Benefits of Ka-band GaN MMIC High Power Amplifiers with Wide Bandwidth and High Spectral/Power Added Efficiencies for Cognitive Radio Platforms," *2023 IEEE Cognitive Communications for Aerospace Applications Workshop (CCAAW)*, Cleveland, OH, June 20–22, 2023.
13. NTIA Manual of Regulations and Procedures for Federal Radio Frequency Management (Redbook), Chap. 5, Section 5.6, Jan 2021 Edition.
14. B. Heying, W.-B. Luo, I. Smorchkova, S. Din, and M. Wojtowicz, "Reliable GaN HEMTs for High Frequency Applications," *IEEE MTT-S Inter. Micro Symp Dig*, pp. 1218–1220, Anaheim, CA, May 23–28, 2010.